Supplementary information

Table of contents

Experimental Measurement Methods

Physical measurements. Differential scanning calorimetry (DSC), variable-temperature single-crystal X-ray diffraction, powder X-ray diffraction (PXRD) measurements, dielectric measurements, ultraviolet-vis spectral measurements and electronic structure calculations were described in Supporting Information.

DSC Measurements.

DSC measurement of $(DPA)_4Bi_2Br_{10}$, $(DPA)_5Pb_2Br_9$ and $(DPA)_4AgBiBr_8$ was carried out in the temperature range from 173 to 453 K at a rate of 20 K min^{-1} using a PerkinElmer Diamond DSC instrument.

Single-Crystal X-ray Crystallography.

Variable-temperature single-crystal XRD data of $(DPA)_4Bi_2Br_{10}$, $(DPA)_5Pb_2Br_9$ and $(DPA)_4AgBiBr_8$ were collected using a Bruker APEX-II CCD with Mo Kα radiation (λ = 0.71073 Å) at different temperature, whose processing was disposed by the APEX3. Variable-temperature crystal structures were solved using a direct method and subsequent continuous Fourier synthesis. Subsequently, these crystals were refined by full-matrix leastsquares methods based on F2 using the SHELXTL software package. Eventually, in addition to the asymmetric units and packing shown in main body using DIAMOND software, other relevant crystallographic data and structure refinement are listed in **Table S1** and **S2** in supporting information.

Solid-state NMR measurements.

Like the synthesis of $(DPA)_4AgBiBr_8$, in the synthesis process, HBr acid (AR≥40%, 10 ml) was replaced with DBr (48% w/w in D_2O, 99+%, 10 g). Eventually, the yellow block crystals of $(DPA-d_3)_4AgBiBr_8$ for single-crystal XRD were obtained after slow cooling.

Wide-line ^2H NMR studies were performed by using a Bruker Avance III 300 spectrometer operating at 46.07 MHz. The ^2H spectra were recorded by using a Bruker two-channel static polarization enhancement (PE) probe with a homemade 2.5 mm coil. The spectra were acquired by using a solid echo pulse sequence with a pulse width of 2 μs at a radio-frequency (RF) amplitude of $\gamma B_1/2\pi$ = 125 kHz. The refocusing delay τ

was approximately 30 µs. The ^{2}H spectra were simulated by using the weblab software (https://weblab2.mpip-mainz.mpg.de/weblab66/weblab.html).

The equations for calculation of the spontaneous strain.

For $mmm\mathrm{F}\bar{1}$, the spontaneous strain tensor can be calculated by the following matrix:

$$\varepsilon_{ij} = \begin{bmatrix} \frac{a_{RTP}}{a_{HTP}}\sin\gamma_{RTP} - 1 & \frac{1}{2}\left(\frac{a_{RTP}}{a_{HTP}}\cos\gamma_{RTP}\right) & \frac{1}{2}\left(-\frac{c_{RTP}\sin\alpha_{RTP}\cos(180° - \beta_{RTP})}{c'_{HTP}}\right) \\ \frac{1}{2}\left(\frac{a_{RTP}}{a_{HTP}}\cos\gamma_{RTP}\right) & \frac{b_{RTP}}{b'_{HTP}} - 1 & \frac{1}{2}\left(\frac{c_{RTP}\cos\alpha_{RTP}}{c'_{HTP}}\right) \\ \frac{1}{2}\left(-\frac{c_{RTP}\sin\alpha_{RTP}\cos(180° - \beta_{RTP})}{c'_{HTP}}\right) & \frac{1}{2}\left(\frac{c_{RTP}\cos\alpha_{RTP}}{c'_{HTP}}\right) & \frac{c_{RTP}\sin\alpha_{RTP}\sin(180° - \beta_{RTP})}{c'_{HTP}} - 1 \end{bmatrix}$$

The total spontaneous strain ε_{ss} can be calculated by $\varepsilon_{ss} = \sqrt{\sum_{ij}\varepsilon_{ij}^2}$.

Density Functional Theory Calculations.

Density functional theory (DFT) were performed with the Vienna Ab Initio Simulation Package (VASP)[1]. The Perdew−Burke−Ernzerhof(PBE)[2] functional and frozen-core all electron projector augmented wave (PAW)[3] model was employed. The cutoff energy was set to 500 eV. And the convergence criteria for the residual force and energy on each atom during structure relaxation were set to 0.01 eV/Å and 10^{-5} eV, respectively.
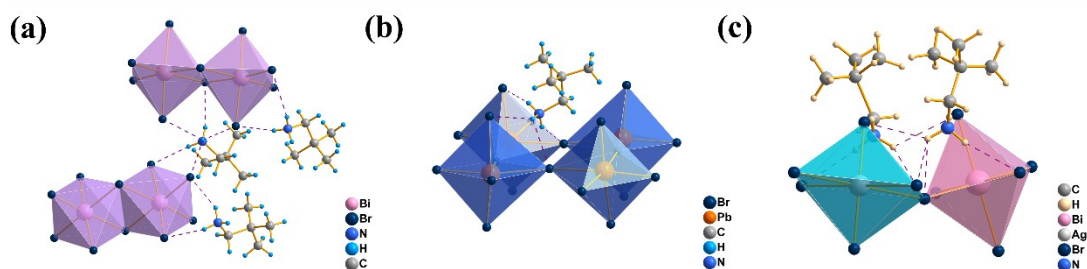
Figure S1. Hydrogen bonds of **(DPA)$_4$Bi$_2$Br$_{10}$** (a), **(DPA)$_5$Pb$_2$Br$_9$** (b) and **(DPA)$_4$AgBiBr$_8$** (c).
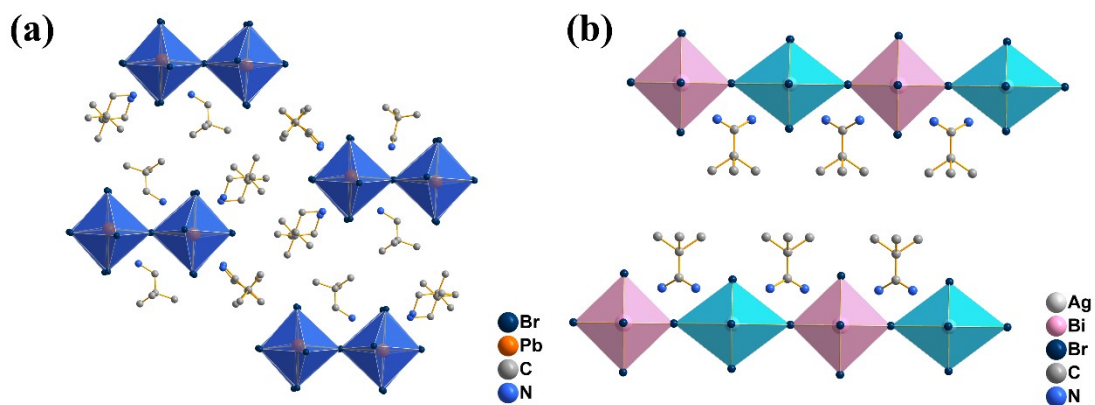
Figure S2. Packing diagram of compound **(DPA)₅Pb₂Br₉** (a) and **(DPA)₄AgBiBr₈** (b) at high temperature.
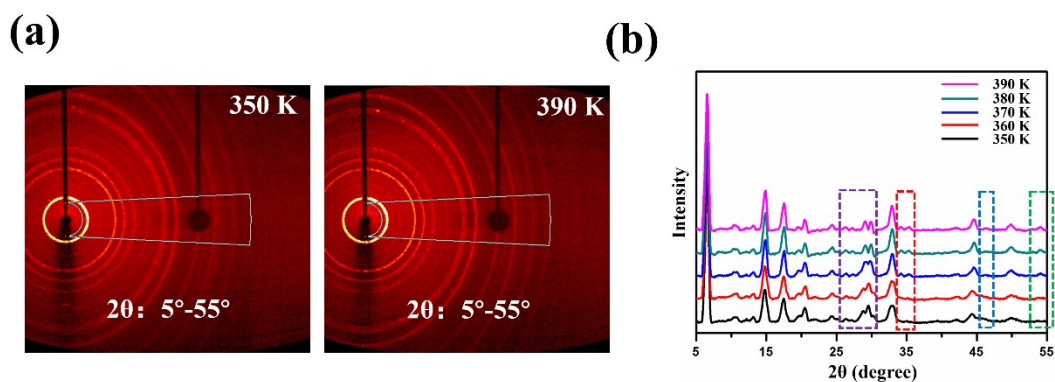
Figure S3. (a) Two-dimensional powder diffraction pattern of **(DPA)₄AgBiBr₈** before (350 K) and after (390 K) phase transition temperature. (b) Variable-temperature powder X-ray diffraction patterns of **(DPA)₄AgBiBr₈** from 350 K to 390 K.
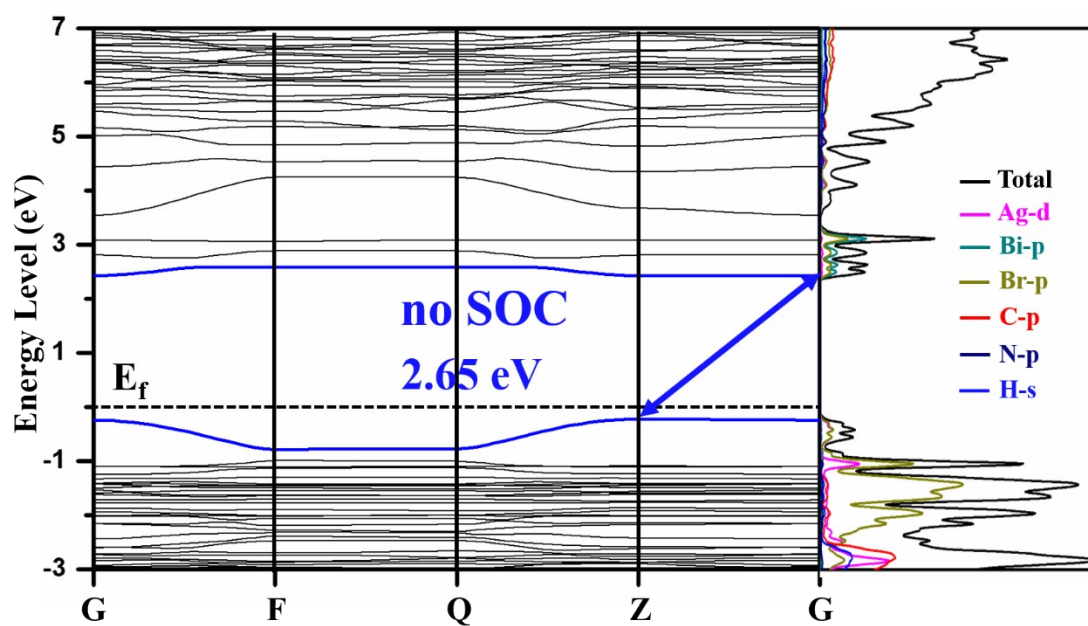
Figure S4. Calculated energy band structure of **(DPA)$_4$AgBiBr$_8$** without spin-orbit coupling (SOC), and corresponding partial density of states (PDOS).
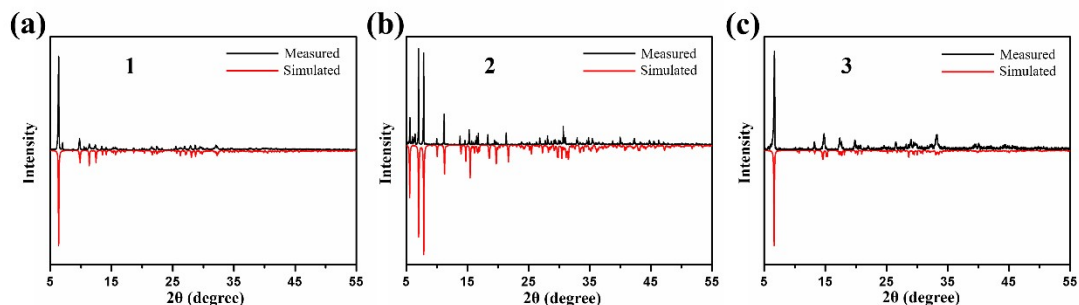
Figure S5. Measured and simulated powder X-ray diffraction patterns of **(DPA)$_4$Bi$_2$Br$_{10}$, (DPA)$_5$Pb$_2$Br$_9$** and **(DPA)$_4$AgBiBr$_8$**.
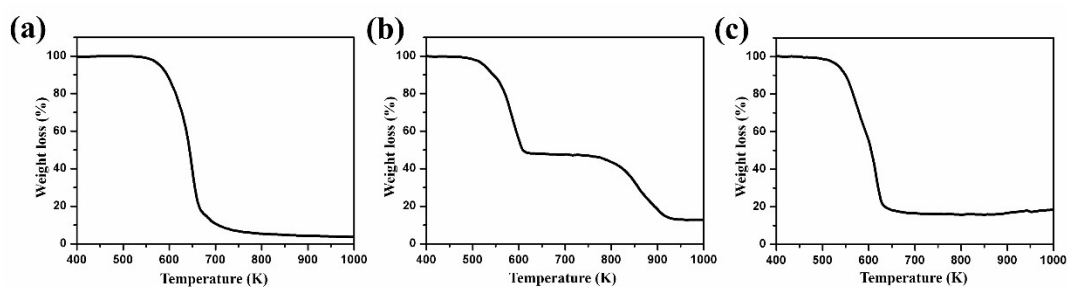
Figure S6. TGA curve of **(DPA)$_4$Bi$_2$Br$_{10}$, (DPA)$_5$Pb$_2$Br$_9$** and **(DPA)$_4$AgBiBr$_8$**.

Table S1. Crystal data and structure refinements for **(DPA)$_4$Bi$_2$Br$_{10}$, (DPA)$_5$Pb$_2$Br$_9$** and **(DPA)$_4$AgBiBr$_8$**.

	(DPA)$_4$Bi$_2$Br$_{10}$ 200 K	(DPA)$_5$Pb$_2$Br$_9$ 273 K	(DPA)$_4$AgBiBr$_8$ 150 K
Empirical formula	C$_{20}$H$_{56}$Bi$_2$Br$_{10}$N$_4$	C$_{25}$H$_{70}$Br$_9$N$_5$Pb$_2$	C$_{20}$H$_{56}$AgBiBr$_8$N$_4$
Formula weight	1569.74	1574.43	1308.74
Crystal system	Triclinic	Triclinic	Triclinic
Space group	$P\bar{1}$	$P\bar{1}$	$P\bar{1}$
a (Å)	12.4378(19)	11.975 (2)	8.4797(6)
b (Å)	13.2166(19)	13.366 (2)	8.7683(6)
c (Å)	14.021(3)	17.472 (3)	13.9411(9)
α (°)	97.835(4)	72.618 (5)	73.253(3)
β (°)	93.139(5)	70.213 (4)	88.908(3)
γ (°)	90.289(4)	77.258 (4)	87.415(3)
Volume(Å^3)	2279.7(6)	2488.9 (8)	991.56(12)
Z	2	2	1
Radiation type	MoK\a	MoK\a	MoK\a
Absorption correction	Multi-scan	Multi-scan	Multi-scan
D$_{calc}$ /g cm^{-3}	2.287	2.101	2.192

F (000)	1440	1468	614	
GOF	1.022	1.052	1.095	
$R_1[I > 2\sigma(I)]$	0.0492	0.0658	0.1097	
w$R2[I > 2\sigma(I)]$	0.1202	0.2002	0.3188	

Table S2. Selected bond lengths [Å] and bond angles [°] for **(DPA)$_4$Bi$_2$Br$_{10}$** at 200 K.

Temperature	bond lengths [Å]		bond angles [°]	
200 K	Bi01—Br0B	2.7076 (12)	Br0B—Bi01—Br0A	93.49 (4)
	Bi01—Br0A	2.7782 (10)	Br0B—Bi01—Br06	92.43 (3)
	Bi01—Br06	2.7841 (9)	Br0A—Bi01—Br06	88.32 (3)
	Bi01—Br05	2.9184 (10)	Br0B—Bi01—Br05	92.84 (3)
	Bi01—Br07	3.0015 (10)	Br0A—Bi01—Br05	92.31 (3)
	Bi01—Br07^i	3.0754 (12)	Br06—Bi01—Br05	174.64 (3)
	Bi02—Br0C	2.6995 (13)	Br0B—Bi01—Br07	88.79 (3)
	Bi02—Br04	2.7749 (10)	Br0A—Bi01—Br07	177.32 (3)
	Bi02—Br09	2.7862 (10)	Br06—Bi01—Br07	90.17 (3)
	Bi02—Br03	2.9298 (10)	Br05—Bi01—Br07	88.99 (3)
	Bi02—Br08	3.0014 (10)	Br0B—Bi01—Br07^i	175.47 (3)
	Bi02—Br08^{ii}	3.0951 (12)	Br0A—Bi01—Br07^i	90.91 (3)
			Br06—Bi01—Br07^i	88.78 (3)
			Br05—Bi01—Br07^i	85.88 (3)
			Br07—Bi01—Br07^i	86.84 (3)
			Br0C—Bi02—Br04	92.77 (3)
			Br0C—Bi02—Br09	94.29 (4)
			Br04—Bi02—Br09	87.72 (3)
			Br0C—Bi02—Br03	91.93 (3)
			Br04—Bi02—Br03	175.27 (3)
			Br09—Bi02—Br03	92.48 (3)
			Br0C—Bi02—Br08	89.79 (3)
			Br04—Bi02—Br08	88.60 (3)
			Br09—Bi02—Br08	174.64 (3)
			Br03—Bi02—Br08	90.87 (3)
			Br0C—Bi02—Br08^{ii}	174.98 (3)
			Br04—Bi02—Br08^{ii}	88.21 (3)
			Br09—Bi02—Br08^{ii}	90.67 (3)
			Br03—Bi02—Br08^{ii}	87.06 (3)
			Br08—Bi02—Br08^{ii}	85.31 (3)
			Bi01—Br07—Bi01^i	93.16 (3)
			Bi02—Br08—Bi02^{ii}	94.69 (3)

Symmetry codes: (i) −x, −y+1, −z+1; (ii) −x+1, −y+2, −z+1. (200 K)

Table S3. Selected bond lengths [Å] and bond angles [°] for **(DPA)$_5$Pb$_2$Br$_9$** at 273 and 310 K.

Temperature	bond lengths [Å]		bond angles [°]	
273 K	Br1—Pb1	3.1158 (13)	Pb1—Br1—Pb2[i]	162.60 (6)
	Br1—Pb2[i]	3.1851 (14)	Pb1—Br5—Pb2	168.15 (5)
	Br2—Pb1	3.0801 (15)	Pb2—Br8—Pb1[ii]	151.29 (4)
	Br3—Pb1	2.9570 (13)	Br4—Pb1—Br3	89.97 (4)
	Br4—Pb1	2.9458 (13)	Br4—Pb1—Br5	95.53 (4)
	Br5—Pb1	3.0082 (12)	Br3—Pb1—Br5	98.38 (4)
	Br5—Pb2	3.0278 (12)	Br4—Pb1—Br2	174.73 (4)
	Br6—Pb2	2.9032 (13)	Br3—Pb1—Br2	85.87 (4)
	Br7—Pb2	3.1475 (15)	Br5—Pb1—Br2	88.27 (4)
	Br8—Pb2	3.0773 (12)	Br4—Pb1—Br8[iii]	85.37 (4)
	Br8—Pb1[ii]	3.0918 (12)	Br3—Pb1—Br8[iii]	90.98 (4)
	Br9—Pb2	2.8852 (15)	Br5—Pb1—Br8[iii]	170.59 (3)
			Br2—Pb1—Br8[iii]	91.47 (4)
			Br4—Pb1—Br1	92.79 (4)
			Br3—Pb1—Br1	175.45 (4)
			Br5—Pb1—Br1	84.96 (4)
			Br2—Pb1—Br1	91.18 (4)
			Br8[iii]—Pb1—Br1	85.64 (4)
			Br9—Pb2—Br6	90.43 (4)
			Br9—Pb2—Br5	95.91 (4)
			Br6—Pb2—Br5	95.66 (4)
			Br9—Pb2—Br8	91.03 (4)
			Br6—Pb2—Br8	89.88 (4)
			Br5—Pb2—Br8	171.07 (3)
			Br9—Pb2—Br7	173.83 (4)
			Br6—Pb2—Br7	84.29 (4)
			Br5—Pb2—Br7	87.81 (4)
			Br8—Pb2—Br7	85.78 (4)
			Br9—Pb2—Br1[i]	99.62 (4)
			Br6—Pb2—Br1[i]	169.26 (4)
			Br5—Pb2—Br1[i]	87.13 (4)
			Br8—Pb2—Br1[i]	86.17 (4)
			Br7—Pb2—Br1[i]	85.46 (4)
310 K	Br1—Pb2	3.0715 (12)	Pb2—Br1—Pb1[i]	152.03 (5)
	Br1—Pb1[i]	3.0862 (12)	Pb1—Br2—Pb2	168.88 (6)
	Br2—Pb1	3.0189 (12)	Pb1—Br6—Pb2[ii]	164.86 (6)
	Br2—Pb2	3.0338 (12)	Br3—Pb1—Br4	90.34 (4)
	Br3—Pb1	2.9389 (13)	Br3—Pb1—Br2	98.68 (4)
	Br4—Pb1	2.9554 (14)	Br4—Pb1—Br2	95.44 (4)
	Br5—Pb2	2.8957 (13)	Br3—Pb1—Br8	85.54 (4)

Br6—Pb1	3.1315 (13)	Br4—Pb1—Br8	174.65 (4)
Br6—Pb2^{ii}	3.1833 (14)	Br2—Pb1—Br8	88.57 (4)
Br7—Pb2	2.9059 (15)	Br3—Pb1—Br1^{iii}	90.72 (4)
Br8—Pb1	3.0852 (15)	Br4—Pb1—Br1^{iii}	85.72 (4)
Br9—Pb2	3.1416 (16)	Br2—Pb1—Br1^{iii}	170.51 (4)
		Br8—Pb1—Br1^{iii}	90.91 (4)
		Br3—Pb1—Br6	174.77 (4)
		Br4—Pb1—Br6	92.63 (4)
		Br2—Pb1—Br6	85.33 (4)
		Br8—Pb1—Br6	91.22 (4)
		Br1^{iii}—Pb1—Br6	85.21 (4)
		Br5—Pb2—Br7	90.45 (4)
		Br5—Pb2—Br2	96.40 (4)
		Br7—Pb2—Br2	95.90 (4)
		Br5—Pb2—Br1	89.68 (4)
		Br7—Pb2—Br1	90.49 (4)
		Br2—Pb2—Br1	171.13 (4)
		Br5—Pb2—Br9	84.45 (5)
		Br7—Pb2—Br9	173.93 (4)
		Br2—Pb2—Br9	87.96 (4)
		Br1—Pb2—Br9	86.20 (4)
		Br5—Pb2—Br6^{ii}	170.20 (4)
		Br7—Pb2—Br6^{ii}	98.19 (4)
		Br2—Pb2—Br6^{ii}	87.35 (4)
		Br1—Pb2—Br6^{ii}	85.65 (4)
		Br9—Pb2—Br6^{ii}	86.64 (4)

Symmetry codes: (i) $-x+1, -y+1, -z+1$; (ii) $x-1, y, z$; (iii) $x+1, y, z$. (273 K)
Symmetry codes: (i) $x-1, y, z$; (ii) $-x+1, -y+1, -z+1$; (iii) $x+1, y, z$. (310 K)

Table S4. Selected bond lengths [Å] and bond angles [°] for **(DPA)$_4$AgBiBr$_8$** at 150 and 375 K.

Temperature	bond lengths [Å]		bond angles [°]	
150 K	Bi1—Br1^i	2.827 (2)	Br1^i—Bi1—Br1	180.0
	Bi1—Br1	2.827 (2)	Br1^i—Bi1—Br3	92.26 (7)
	Bi1—Br3	2.8347 (19)	Br1—Bi1—Br3	87.74 (7)
	Bi1—Br3^i	2.8348 (19)	Br1^i—Bi1—Br3^i	87.74 (7)
	Bi1—Br2^i	2.873 (2)	Br1—Bi1—Br3^i	92.26 (7)
	Bi1—Br2	2.873 (2)	Br3—Bi1—Br3^i	180.00 (8)
	Ag1—Br4^{ii}	2.547 (3)	Br1^i—Bi1—Br2^i	88.43 (11)

S8

	Ag1—Br4	2.547 (3)	Br1—Bi1—Br2^i	91.57 (11)
			Br3—Bi1—Br2^i	91.07 (7)
			Br3^i—Bi1—Br2^i	88.93 (7)
			Br1^i—Bi1—Br2	91.57 (11)
			Br1—Bi1—Br2	88.43 (11)
			Br3—Bi1—Br2	88.93 (7)
			Br3^i—Bi1—Br2	91.07 (7)
			Br2^i—Bi1—Br2	180.0
			Br4^{ii}—Ag1—Br4	180.0
375 K	Ag1—Br1^i	2.538 (13)	Br1^i—Ag1—Br1	180.0
	Ag1—Br1	2.538 (13)	Br1^i—Ag1—Br3	90.000 (1)
	Ag1—Br3	3.335 (9)	Br1—Ag1—Br3	90.000 (1)
	Bi1—Br2^{ii}	2.816 (13)	Br2^{ii}—Bi1—Br2	180.0
	Bi1—Br2	2.816 (13)	Br2^{ii}—Bi1—Br3	90.000 (1)
	Bi1—Br3	2.868 (9)	Br2—Bi1—Br3	90.000 (1)
	Bi1—Br3^{ii}	2.868 (9)	Br2^{ii}—Bi1—Br3^{ii}	90.000 (1)
	Bi1—Br3^{iii}	2.868 (9)	Br2—Bi1—Br3^{ii}	90.000 (2)
	Bi1—Br3^{iv}	2.868 (9)	Br3—Bi1—Br3^{ii}	180.0
			Br2^{ii}—Bi1—Br3^{iii}	90.000 (3)
			Br2—Bi1—Br3^{iii}	90.000 (1)
			Br3—Bi1—Br3^{iii}	90.5 (6)
			Br3^{ii}—Bi1—Br3^{iii}	89.5 (5)
			Br2^{ii}—Bi1—Br3^{iv}	90.000 (1)
			Br2—Bi1—Br3^{iv}	90.000 (3)
			Br3—Bi1—Br3^{iv}	89.5 (5)
			Br3^{ii}—Bi1—Br3^{iv}	90.5 (6)
			Br3^{iii}—Bi1—Br3^{iv}	180.0
			Bi1—Br3—Ag1	179.5 (5)

Symmetry codes: (i) −x+1, −y+1, −z+1; (ii) −x+2, −y+2, −z+1; (iii) −x+1, −y+2, −z+1; (iv) x+1, y, z. (150 K)

Symmetry codes: (i) −x, −y+1, −z; (ii) −x+1, −y+1, −z+1; (iii) x, y, −z+1; (iv) −x+1, −y+1, z; (v) −x+1, y, −z+2; (vi) −x+1, y, z; (vii) x, y, −z+2; (viii) −x, y, z; (ix) −x, y, −z+1. (375 K)

Table S5. Hydrogen-bond geometry (Å, °) for **(DPA)$_4$Bi$_2$Br$_{10}$** at 200 K.

D—H$\cdots A$	D—H	H$\cdots A$	$D\cdots A$	D—H$\cdots A$
C9—H9$B\cdots$Br08^{iii}	0.99	3.03	3.835 (14)	139
C00N—H00$P\cdots$Br03	0.99	2.99	3.635 (15)	124
C00N—H00$O\cdots$Br0B	0.99	3.01	3.982 (15)	167
C00M—H00$M\cdots$Br07^{iv}	0.99	2.97	3.787 (14)	141
C3H—H3H2$\cdots$Br0C	0.99	3.04	4.009 (14)	166
C3H—H3H1$\cdots$Br05^{iv}	0.99	3.02	3.659 (14)	123

D—H⋯A	D—H	H⋯A	D⋯A	D—H⋯A
N00G—H00L⋯Br06[iv]	0.91	2.60	3.423 (8)	150
N00G—H00K⋯Br05[v]	0.91	2.74	3.488 (8)	140
N00G—H00K⋯Br04[iii]	0.91	2.97	3.534 (8)	122
N00G—H00J⋯Br09[iii]	0.91	2.61	3.485 (8)	163
N00F—H00I⋯Br0A	0.91	2.71	3.514 (8)	148
N00F—H00H⋯Br06	0.91	2.83	3.503 (8)	132
N00F—H00H⋯Br03[v]	0.91	2.81	3.496 (9)	133
N00F—H00G⋯Br04[iii]	0.91	2.55	3.438 (8)	166
N00E—H00F⋯Br05	0.91	2.44	3.340 (8)	168
N00E—H00E⋯Br0A	0.91	2.99	3.585 (8)	125
N00E—H00E⋯Br04[ii]	0.91	2.93	3.438 (9)	117
N00E—H00E⋯Br03	0.91	2.66	3.333 (8)	131
N00E—H00D⋯Br08	0.91	2.64	3.463 (8)	151
N00D—H00C⋯Br07[iv]	0.91	2.66	3.477 (7)	150
N00D—H00B⋯Br09	0.91	2.96	3.555 (8)	125
N00D—H00B⋯Br06[v]	0.91	2.93	3.478 (8)	120
N00D—H00B⋯Br05[iv]	0.91	2.67	3.326 (7)	130
N00D—H00A⋯Br03	0.91	2.45	3.344 (7)	166

Symmetry codes: (ii) −x+1, −y+2, −z+1; (iii) x, y−1, z; (iv) x+1, y, z; (v) −x+1, −y+1, −z+1.

Table S6. Hydrogen-bond geometry (Å, °) for **(DPA)$_5$Pb$_2$Br$_9$** at 273 K.

D—H⋯A	D—H	H⋯A	D⋯A	D—H⋯A
N5—H5E⋯Br9	0.89	2.63	3.349 (19)	139
N5—H5D⋯Br6	0.89	2.81	3.519 (18)	137
N5—H5D⋯Br3[ii]	0.89	3.07	3.510 (17)	113
N5—H5C⋯Br4[ii]	0.89	2.87	3.396 (15)	120
N5—H5D⋯Br3[ii]	0.89	3.07	3.510 (17)	113
C25—H25A⋯Br9	0.97	2.99	3.570 (12)	120
N4—H4F⋯Br3[iv]	0.89	2.79	3.495 (14)	137
N4—H4E⋯Br7[v]	0.89	3.13	3.852 (13)	139
N4—H4E⋯Br6[v]	0.89	2.81	3.469 (13)	132
N4—H4D⋯Br8[v]	0.89	3.00	3.423 (12)	111
N4—H4D⋯Br2[iv]	0.89	3.03	3.832 (14)	151
N3—H3F⋯Br7[vi]	0.89	3.02	3.893 (15)	167
N3—H3E⋯Br8	0.89	2.99	3.737 (14)	143
N3—H3E⋯Br1[ii]	0.89	2.99	3.441 (12)	114
N3—H3D⋯Br4[ii]	0.89	2.64	3.430 (14)	149
C12—H12B⋯Br9	0.97	3.01	3.951 (17)	164
C12—H12A⋯Br8[vi]	0.97	3.12	3.782 (15)	127
N2—H2F⋯Br2	0.89	2.81	3.605 (14)	150

D—H···A	D—H	H···A	D···A	D—H···A
N2—H2E···Br1	0.89	2.71	3.488 (13)	147
N2—H2D···Br7	0.89	2.85	3.607 (13)	144
N2—H2D···Br1^i	0.89	3.09	3.620 (14)	120
N1—H1C···Br7^{vii}	0.89 (1)	2.73 (2)	3.495 (12)	144 (2)
N1—H1B···Br2^{vii}	0.89 (1)	2.90 (2)	3.430 (15)	120 (2)
C5—H5B···Br2^{vii}	0.97	3.12	3.715 (14)	121

Symmetry codes: (i) −x+1, −y+1, −z+1; (ii) x−1, y, z; (iv) x−1, y−1, z; (v) x, y−1, z; (vi) −x, −y+1, −z+1; (vii) −x+1, −y+2, −z+1.

Table S7. Hydrogen-bond geometry (Å, °) for **(DPA)₄AgBiBr₈** at 150 K.

D—H···A	D—H	H···A	D···A	D—H···A
C7—H7A···Br1	0.99	2.87	3.77 (4)	151
N2—H2C···Br2^i	0.91	2.86	3.70 (2)	154
N2—H2B···Br3^{iii}	0.91	2.84	3.45 (2)	126
N2—H2B···Br1^{iii}	0.91	3.05	3.71 (2)	131
N2—H2A···Br4	0.91	2.66	3.43 (2)	144
N1—H1E···Br3^{iv}	0.91	2.72	3.56 (3)	154
N1—H1D···Br4^{ii}	0.91	2.52	3.34 (3)	150
N1—H1D···Br2^i	0.91	3.25	3.58 (3)	104
N1—H1D···Br1^{iv}	0.91	3.14	3.55 (3)	109
N1—H1C···Br2^{iv}	0.91	3.01	3.65 (3)	129
C1—H1B···Br1^i	0.99	2.97	3.88 (4)	154

Symmetry codes: (i) −x+1, −y+1, −z+1; (ii) −x+2, −y+2, −z+1; (iii) −x+1, −y+2, −z+1; (iv) x+1, y, z.

Table S8. Crystal data and structure refinements for **(DPA)₅Pb₂Br₉** and **(DPA)₄AgBiBr₈** at high temperature phase.

	(DPA)₅Pb₂Br₉ (310 K)	**(DPA)₄AgBiBr₈** (375 K)
Empirical formula	$C_{25}H_{69}Br_9N_5Pb_2$	$C_{20}AgBiBr_8N_8$
Formula weight	1573.42	1308.41
Crystal system	Triclinic	Orthorhombic
Space group	$P\bar{1}$	$Cmmm$
a (Å)	11.996(2)	8.774(10)
b (Å)	13.422(2)	27.47(3)
c (Å)	17.477(3)	8.771(9)
α (°)	72.658(4)	90
β (°)	70.158(4)	90
γ (°)	77.179(4)	90
Volume(Å³)	2503.6(8)	2114(4)
Z	2	2

Radiation type	MoK\a	MoK\a
Absorption correction	Multi-scan	Multi-scan
D_{calc} /g cm^{-3}	2.087	2.056
F (000)	1466	1172
GOF	1.054	1.244
$R_1[I > 2\sigma(I)]$	0.0605	0.1110
w$R2[I > 2\sigma(I)]$	0.1824	0.3235

Table S9. The reported space group and band gap of Ruddlesden−Popper AgBiBr- and AgBiI-based materials (n=1).

Formula	Space group	Band gap (eV)	Ref
$(BA)_4AgBiBr_8$	$C2/m$ (278 K)	2.5	4
	$P2_1/c$ (100 K)		
$(BA)_4AgBiBr_8$	$Bmab$	2.65	5
$(PA)_4AgBiBr_8$	$C2/m$	2.41	6
$(PA)_2CsAgBiBr_7$	$\underline{P2_1/m}$	2.32	6
$(BDA)_4AgBiBr_8$	$P\bar{1}$	2.43	6
$(OcA)_4AgBiBr_8$	$P2/m$	2.45	6
$(DPA)_4AgBiBr_8$	$P\bar{1}$ (150 K)	2.44	this work
	$Cmmm$ (375 K)		
$(IPA)_4AgBiI_8$	$P\bar{1}$	1.87	7
$(3\text{-}IPA)_4AgBiI_8$	$P\bar{1}$	1.87	7
$(4\text{-}AMP)_4AgBiI_8 \cdot H_2O$	$C2_1/c$	2.1	8
$(4\text{-}APP)_4AgBiI_8 \cdot H_2O$	$C2/c$	2.1	8

Appendix S1. Acronyms arranged in top-down order in Table S9.

BA: Butylammonium

PA: Propylammonium

BDA: Butane-1,4-diammonium

OcA: Octylammonium

DPA: 2,2-dimethylpropan-1-aminium

IPA: 3-iodopropan-1-aminium

3-IPA: 3-Iodopropylammonium

4-AMP: 4-(Ammoniomethyl) piperidinium

4-APP: 4-Ammoniumpiperidine

Reference:

(1) Kresse, G.; Furthmüller, J. Efficiency of ab-initio total energy calculations for metals and semiconductors using a plane-wave basis set. *Comput. Mater. Sci.* **1996**, *6*, 15-50.

(2) Perdew, J. P.; Ernzerhof, M.; Burke, K. Rationale for mixing exact exchange with density functional approximations. *J. Chem. Phys.* **1996**, *105*, 9982.

(3) Blöchl, P. E. Projector augmented-wave method. *Phys. Rev. B* **1994**, *50*,

17953-17979.

(4) Connor, B. A.; Leppert, L.; Smith, M. D.; Neaton, J. B.; Karunadasa, H. I. Layered Halide Double Perovskites: Dimensional Reduction of Cs2AgBiBr6. *J. Am. Chem. Soc.* **2018**, *140*, 5235-5240.

(5) McClure, E. T.; McCormick, A. P.; Woodward, P. M. Four Lead-free Layered Double Perovskites with the n = 1 Ruddlesden-Popper Structure. *Inorg. Chem.* **2020**, *59*, 6010-6017.

(6) Mao, L.; Teicher, S. M. L.; Stoumpos, C. C.; Kennard, R. M.; DeCrescent, R. A.; Wu, G.; Schuller, J. A.; Chabinyc, M. L.; Cheetham, A. K.; Seshadri, R. Chemical and Structural Diversity of Hybrid Layered Double Perovskite Halides. *J. Am. Chem. Soc.* **2019**, *141*, 19099-19109.

(7) Yao, Y.; Kou, B.; Peng, Y.; Wu, Z.; Li, L.; Wang, S.; Zhang, X.; Liu, X.; Luo, J. (C3H9NI)4AgBiI8: a direct-bandgap layered double perovskite based on a short-chain spacer cation for light absorption. *Chem. Commun. (Cambridge, U. K.)* **2020**, *56*, 3206-3209.

(8) Lassoued, M. S.; Bi, L.-Y.; Wu, Z.; Zhou, G.; Zheng, Y.-Z. Piperidine-induced Switching of the direct band gaps of Ag(i)/Bi(iii) bimetallic iodide double perovskites. *J. Mater. Chem. C* **2020**, *8*, 5349-5354.